

## Article

# Advanced Stabilization Methods of Plasma Devices for Plasma-Based Acceleration

Mario Galletti <sup>1,2,3\*</sup> , Maria Pia Anania <sup>4</sup>, Sahar Arjmand <sup>4</sup>, Angelo Biagioni <sup>4</sup>, Gemma Costa <sup>4</sup> ,  
Martina Del Giorno <sup>4</sup>, Massimo Ferrario <sup>4</sup>, Valerio Lollo <sup>4</sup>, Riccardo Pompili <sup>4</sup> , Yoav Raz <sup>5</sup> , Vladimir Shpakov <sup>4</sup>,  
Fabio Villa <sup>4</sup> , Arie Zigler <sup>5</sup> and Alessandro Cianchi <sup>1,2,3</sup> 

<sup>1</sup> Department of Physics, Tor Vergata University, Via Ricerca Scientifica 1, 00133 Rome, Italy; alessandro.cianchi@uniroma2.it

<sup>2</sup> INFN-Tor Vergata, Via Ricerca Scientifica 1, 00133 Rome, Italy

<sup>3</sup> NAST Center, Via Ricerca Scientifica 1, 00133 Rome, Italy

<sup>4</sup> Laboratori Nazionali di Frascati, Via Enrico Fermi 54, 00044 Frascati, Italy; maria.pia.anania@lnf.infn.it (M.P.A.); sahar.arjmand@lnf.infn.it (S.A.); angelo.biagioni@lnf.infn.it (A.B.); gemma.costa@lnf.infn.it (G.C.); martina.delgiorno@lnf.infn.it (M.D.G.); massimo.ferrario@lnf.infn.it (M.F.); valerio.lollo@lnf.infn.it (V.L.); riccardo.pompili@lnf.infn.it (R.P.); vladimir.shpakov@lnf.infn.it (V.S.); fabio.villa@lnf.infn.it (F.V.)

<sup>5</sup> Racah Institute of Physics, Hebrew University, Jerusalem 91904, Israel; yoav.raz@mail.huji.ac.il (Y.R.); arie.zigler@mail.huji.ac.il (A.Z.)

\* Correspondence: mario.galletti@lnf.infn.it

**Abstract:** Towards the next generation of compact plasma-based accelerators, useful in several fields, such as basic research, medicine and industrial applications, a great effort is required to control the plasma creation, the necessity of producing a time-jitter free channel, and its stability namely uniformity and reproducibility. In this *Letter*, we describe an experimental campaign adopting a gas-filled discharge-capillary where the plasma and its generation are stabilized by triggering its ignition with an external laser pulse or an innovative technique based on the primary dark current (DC) in the accelerating structure of a linear accelerator (LINAC). The results show an efficient stabilization of the discharge pulse and plasma density with both pre-ionizing methods turning the plasma device into a symmetrical stable accelerating environment, especially when the external voltage is lowered near the breakdown value of the gas. The development of tens of centimeter long capillaries is enabled and, in turn, longer acceleration lengths can be adopted in a wide range of plasma-based acceleration experiments.

**Keywords:** plasma channels; plasma instabilities; low-energy ns-lasers



**Citation:** Galletti, M.; Anania, M.P.; Arjmand, S.; Biagioni, A.; Costa, G.; Del Giorno, M.; Ferrario, M.; Lollo, V.; Pompili, R.; Raz, Y.; et al. Advanced Stabilization Methods of Plasma Devices for Plasma-Based Acceleration. *Symmetry* **2022**, *14*, 450. <https://doi.org/10.3390/sym14030450>

Academic Editor: Fabio Sattin

Received: 24 January 2022

Accepted: 22 February 2022

Published: 24 February 2022

**Publisher's Note:** MDPI stays neutral with regard to jurisdictional claims in published maps and institutional affiliations.



**Copyright:** © 2022 by the authors. Licensee MDPI, Basel, Switzerland. This article is an open access article distributed under the terms and conditions of the Creative Commons Attribution (CC BY) license (<https://creativecommons.org/licenses/by/4.0/>).

## 1. Introduction

Plasma wakefield acceleration, proposed by Tajima and Dawson [1] in 1979, is able to provide accelerating fields of tens of GV/m, orders of magnitude larger than RF-based ones, so it has been able to attract a lot of attention during the last few decades. Such an acceleration gradient allows to build ultra-compact accelerators suitable in a wide range of applications involving advanced radiation sources based on Free Electron Lasers (FEL) [2–4], Compton scattering [5], and THz radiation [6]. In addition, medical applications, as, for instance, therapy based on so-called FLASH therapy [7] can benefit from compact small accelerators. Moreover, recent works also demonstrated the feasibility to implement plasma-based setup suitable for beam transport as focusing devices producing huge fields of the order of kT/m [8], produced by the discharge flowing through the plasma [9], and able to squeeze the beam size down to few microns [10]. Such remarkable accelerations are produced by the plasma wake, excited by a *driver* pulse, namely, an intense laser pulse (LWFA [11–15]) or a relativistic particle beam (PWFA [16–18]). The resulting wakefield is subsequently adopted to accelerate a trailing *witness* bunch. The latter has several advantages as it is not limited by diffraction nor

dephasing, making possible large acceleration lengths [19–21]. Several techniques are currently employed to generate the plasma channel starting from neutral gas, namely, using an high-voltage (HV) discharge [22] or a laser pulse [23]. However, the plasma, dynamically produced shot-by-shot with a lifetime of about few tens of microseconds [24], suffers from stability and reproducibility issues that are key features to perform stable acceleration experiments or plasma sections, not affected by large jitters, to transport electron bunches. In this *Letter*, we present experimental proof of plasma parameters stabilization adopting two different gas pre-ionizing techniques, one based on triggering by an external laser source, and the other on the generated primary LINAC dark current. The results show that, by pre-ionizing the gas, the resulting shot-to-shot plasma parameters fluctuations are reduced. The stabilization regarding both the discharge waveform and the minimization of the time-jittering is highlighted. They succeeded to turn the plasma device into a symmetrical stable accelerating environment even when the starting configuration is an highly unstable non-symmetrical one (namely, when the external voltage is lowered near the breakdown value of the gas) not able to perform high-quality stable plasma-based acceleration. Finally, the triggering methods are able to produce very stable plasma, being a great advantage in a wide range of plasma-based experiments [10].

## 2. Experimental Setup

The experimental campaign has been carried out at the SPARC\_LAB test facility [25] using a 3 cm long hydrogen gas-filled capillary discharge. The experimental setup is shown in Figure 1.

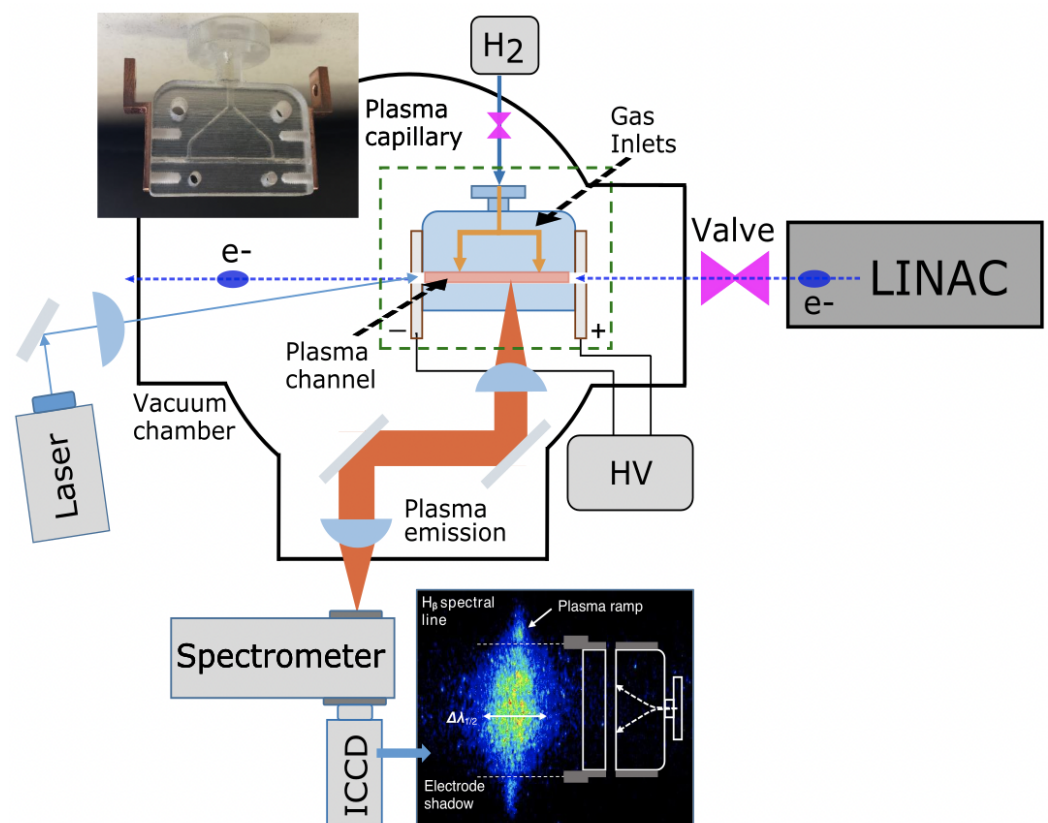


**Figure 1.** Experimental setup. The incoming bunch is focused by a triplet of permanent-magnet quadrupoles (PMQ) into the plasma accelerator module. A second triplet of PMQs is used to extract and transport the bunch up to the diagnostics station. A 3 cm long 3D-printed capillary adopts two symmetric inlets and two electrodes at its ends, connected with the HV source, to produce the full ionization. A pre-ionization laser is focused at the negative electrode spot. The plasma emission is then transported into an imaging spectrometer to allow the effective plasma density retrieval through Stark-broadening technique.

The SPARC\_LAB photo-injector consists of a 1.6-cell S-band electron gun, followed by two 3 m long S-band acceleration sections and one 1.3 m C-band section. The beam is generated directly from the photo-cathode using laser-comb technique [26] by illuminating it with ultra-short laser pulses (130 fs, rms). The first section of the photo-injector is also used as bunch compressor by means of the velocity-bunching technique [27], thus allowing to both accelerate and compress the beam, making the photo-injector very compact. Moreover, it allows precisely adjusting the bunch duration [28] and there is no loss of charge. The plasma experimental setup, depicted in Figure 1, is installed downstream of the photo-injector. It consists of a 3 cm long, 1 mm diameter, 3D-printed capillary filled with hydrogen gas by means of two symmetrical positioned inlets, respectively, located at 1/4 and 3/4 of the structure length. The gas, produced by an electrolytic generator, is injected at a rate of 1 Hz. The gas injection is controlled by a fast electro-valve set with 3 ms aperture time, able to fulfill the experimental requirements. Moreover, the pressure inside the capillary is monitored, and it is of the order of 10–15 mbar. At the capillary opposite ends, two electrodes are positioned and connected with a HV discharge pulsar able to provide up to 600 A current with 20 kV voltage [29] modeling the plasma parameters as required experimentally. The vacuum chamber, as depicted in Figure 1, hosts both the capillary and electro-valve in an environment operating at  $10^{-5}$  mbar. For the gas pre-ionization method based on laser, a 532 nm laser delivering 5 ns pulses with few hundreds of  $\mu\text{J}$  energy is used. The laser focus corresponds with the channel entrance at the first electrode. The plasma radiation is then transported into a SpectraPro-275 imaging spectrometer equipped with an Andor iSTAR-320 intensified camera. By means of this setup, the longitudinal plasma density profile is retrieved by employing a Stark-broadening spectroscopic technique [30–33], by monitoring the  $H_{\beta}$  line, as shown in Figure 1. The proper timing for injection of the beam into the plasma is adjusted by changing the synchronization between the discharge and the beam and is measured using Stark-broadening based diagnostics.

### 3. Results and Discussion

Optimized and controlled plasma discharge can be achieved. The optimization technique is based on the creation of initial free electrons achieved by pre-ionizing the gas either with a laser pulse [34,35] or with the primary dark current in the accelerating structure of a LINAC. Initially, the plasma channel has been fully characterized without any pre-ionizing methods. The plasma density and current are shown in Figures 2 and 3.

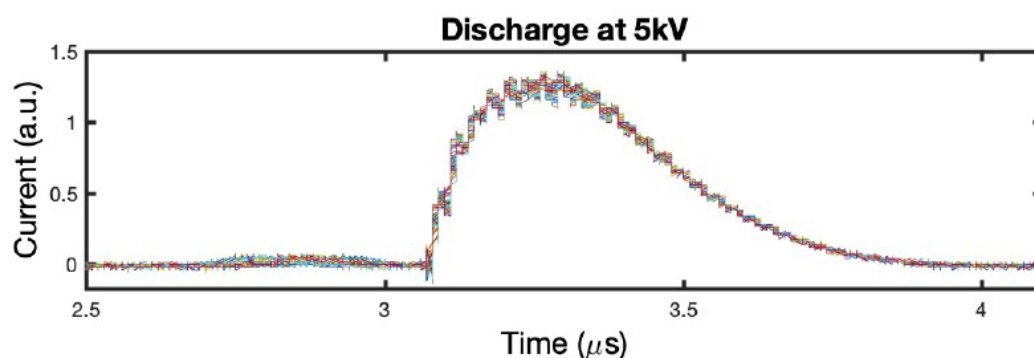


**Figure 2.** Non-stabilized plasma measurement. Plasma discharge waveforms (50 sets) measurements obtained with the stabilization turned off for 5 kV discharge value between the capillary electrodes.

Figure 2 shows a voltage scan of the current waveform acquired by a digital scope. We can clearly see a large shot-to-shot instability on the plasma current shape and peak values, mostly for the 5 kV and 6 kV HV discharge configuration. This difference between low-voltage and high-voltage is quite clear, it is the effect of the full-ionization reached thanks to the higher voltage. However, as previously highlighted, it is important to have an efficient and stable plasma section, especially when the external voltage is lowered near

the breakdown value of the gas enabling the development of very long capillaries and, in turn, acceleration lengths. Finally, it is noticeable, besides the variation of the current amplitude peak, a time-jitter of hundreds nanoseconds of its starting time respect to the fixed stable trigger signal. To go more into detail, the current instability could be blamed on the statistical process of creating free electrons, that can not be controlled, and in turn this implies a significant shot-to-shot variation of the breakdown delay time.

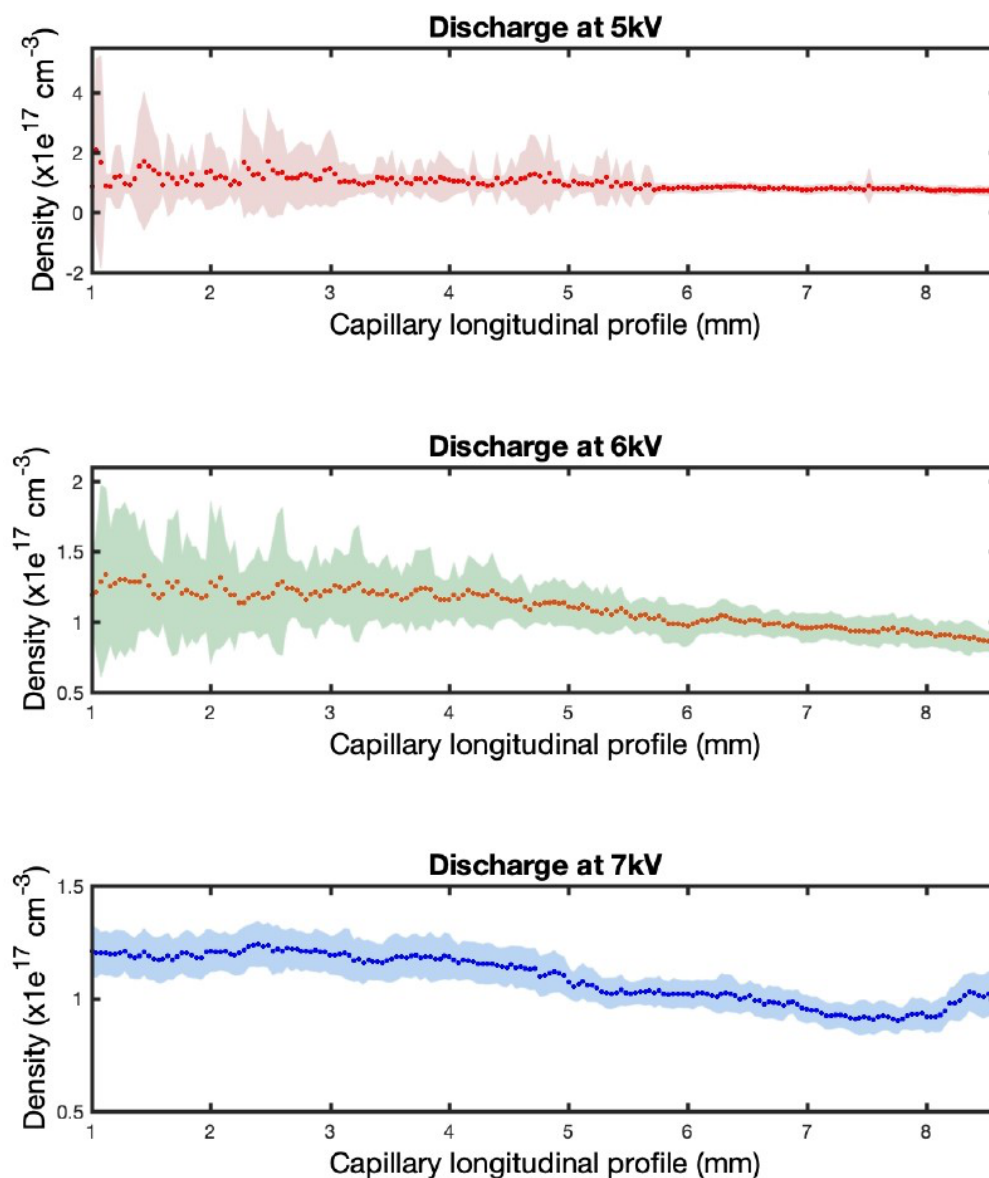
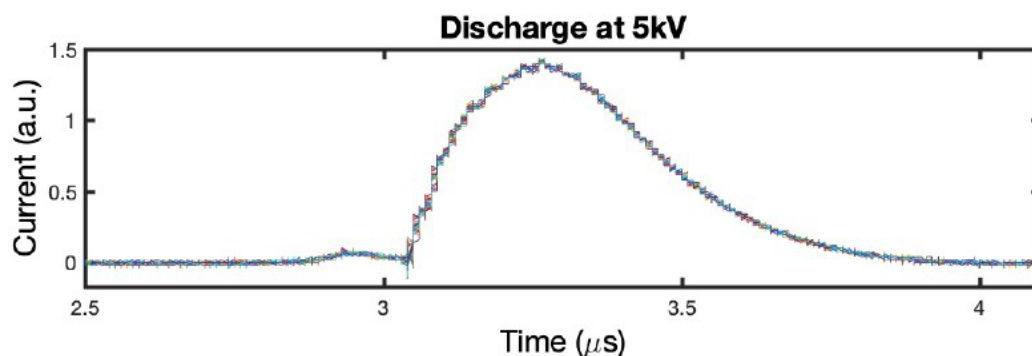


**Figure 3.** Non-stabilized plasma measurement. Plasma longitudinal density profiles measurements obtained with the stabilization turned off for different discharge value. The density profiles extend for 9 mm, a fraction of the capillary. Each plot shows a set of 50 measurements obtained by applying 5–7 kV between the capillary electrodes.

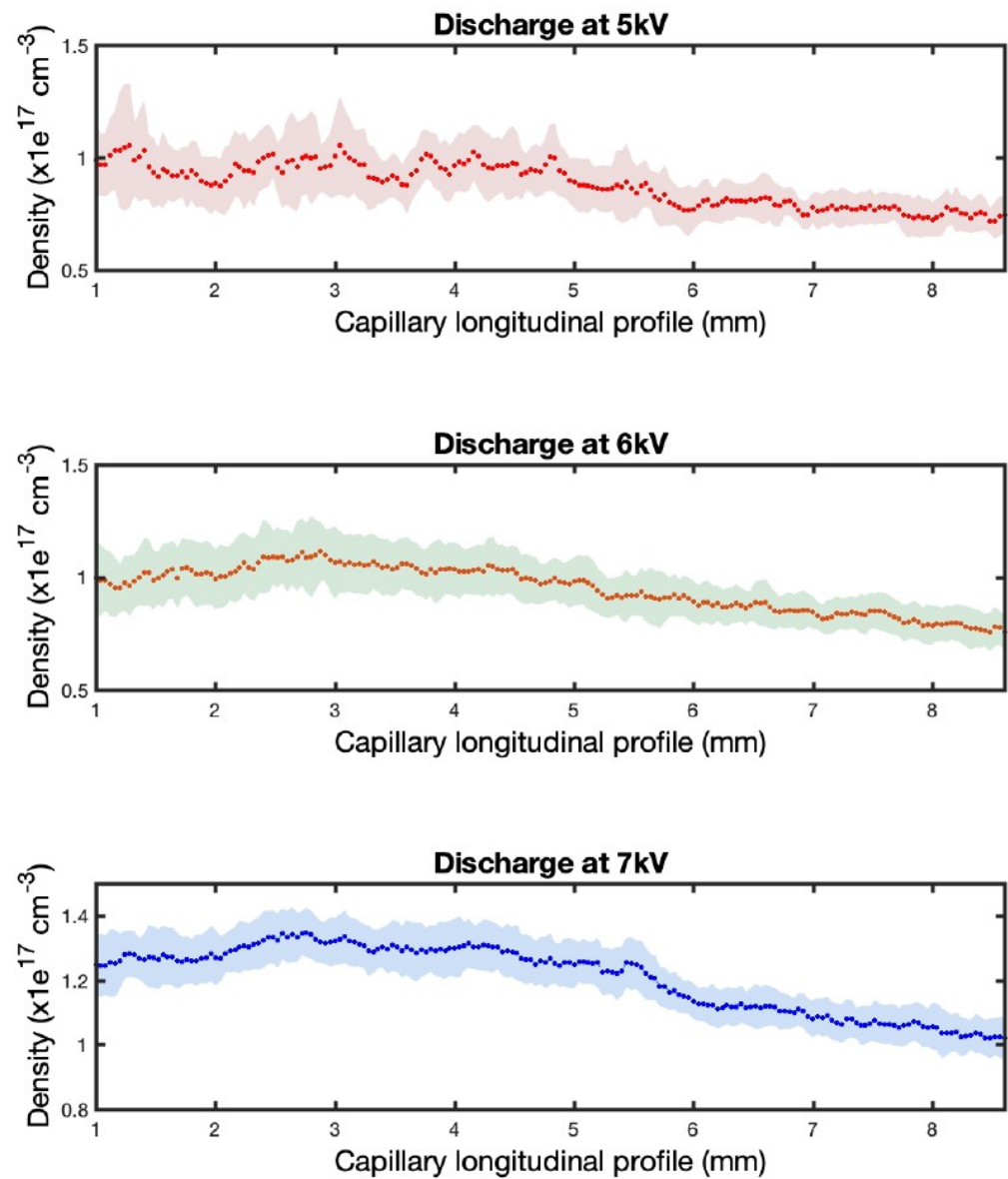
Figure 3 shows a voltage scan of the density longitudinal profile acquired by the Stark system described in the previous section. Indeed, the resulting longitudinal plasma density profile shows strong irregular oscillations especially in the central part of the capillary (corresponding to the 0 mm to 4 mm position of the capillary longitudinal profile). At the capillary opposite the ends where the electrodes are placed, the density decreases and continues to decrease in the plasma plumes just outside the capillary. This plasma density behavior occurs because the gas is escaping from the storing structure. As is noticeable from

Figure 3, the density range reached within the capillary is  $0.5\text{--}2 \times 10^{17} \text{ cm}^{-3}$ . The reported error bars represent the rms deviation calculated by using 50 measured density profiles. Considering the capillary configurations with the discharge at 5 and 6 kV, the plasma density overall shot-to-shot stability is approximately 20% meaning unstable operations, while, for 7 kV configuration the instability drops to  $\sim 10\%$  but still not an optimized operation. These measurements highlight the need of a specific technique to adequately control the plasma channel parameters. A clear enhancement of the plasma stabilization operated by two different triggering techniques providing smaller fluctuations on density, plasma discharge and its time-jitter (corresponding to the ones showed in Figures 2 and 3 in the 5–7 kV voltage range), are presented. Adopting pre-ionizing methods, the resulting stabilization is undeniable when a low-voltage discharge is adopted as in our experimental campaign. Considering the literature and the parameters of our experimental setup namely 3 cm long, 1 mm diameter capillary filled by Hydrogen at 10 mbar, the breakdown voltage is approximately 1 kV according to the Paschen law [36]. In turn, applying a 5 kV voltage, the plasma is rather unstable as experimentally retrieved because such a value is close to the breakdown one. Meanwhile, it is noticeable that ramping up the voltage ( $\sim 7$  kV) the plasma properties become more stable as shown in Figure 3. The laser-triggering method implies the use of a laser with an energy in the 100  $\mu\text{J}$  range and approximately 1 mm spot size at the capillary entrance where the electrode is positioned. The corresponding laser intensity is of the order of  $2.5 \text{ MW/cm}^2$ . The optimization of the triggering technique has been performed varying the pulse energy in the 100  $\mu\text{J}$  to 40 mJ range. Within this energy interval, we did not notice any difference in the plasma parameters stability. Therefore, the lowest energy was set. Such low-intensity pulses, besides efficiently stabilizing the plasma environments, do not significantly decrease the lifetime of the plasma-based device as they are below the damage threshold. Meanwhile, the DC-triggering method does not need any additional devices but it is internally generated by the LINAC. The dark current value corresponding to 70–15 pC range has been measured.

In Figures 4 and 5, we present the characterization of the plasma and discharge parameters influenced by the pre-ionizing techniques. Adopting the presented techniques, the discharge waveform becomes very stable as shown in Figure 4. For sake of completeness, we have to highlight that the trigger/laser signal coming from a photo-diode installed outside the vacuum chamber is arriving at around 3  $\mu\text{s}$ . The RMS amplitude instability is now minimized to the Amperes-level ( $\sim 1$  A) and its rising edge time-jittering is of the order of few nanoseconds ( $\sim 2$  ns).



**Figure 4.** Stabilized plasma measurement. Plasma discharge waveforms (50 sets) measurements obtained with both the pre-ionizing methods for 5 kV discharge value between the capillary electrodes.



**Figure 5.** Stabilized plasma measurement. Plasma longitudinal density profiles measurements obtained with both the pre-ionizing methods for different discharge value. The density profiles extend for 9 mm, a fraction of the capillary. Each plot shows a set of 50 measurements obtained by applying 5–7 kV between the capillary electrodes.

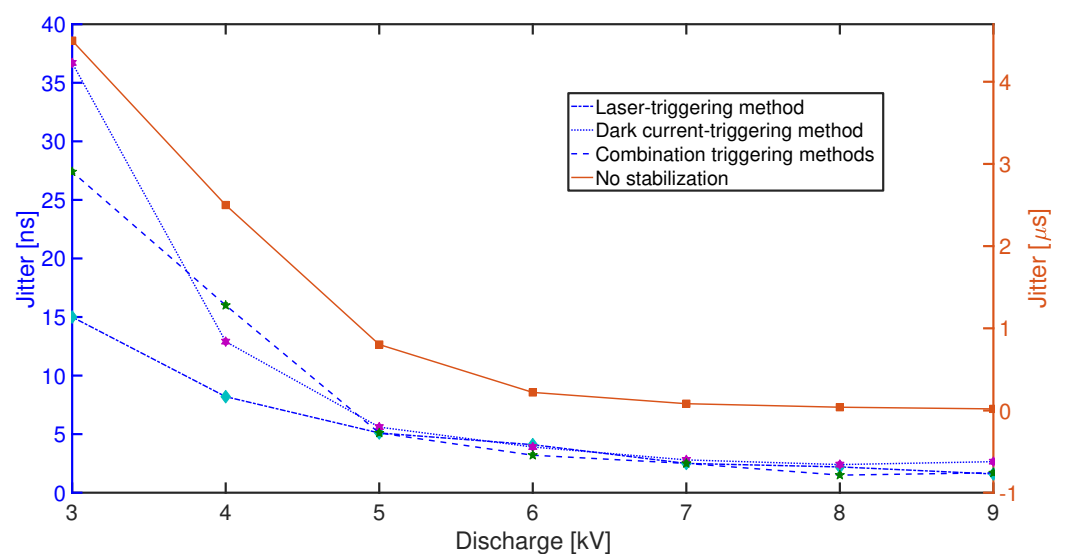
Triggering the discharge, undeniably improves the shot-to-shot stability and the longitudinal uniformity of the resulting plasma profile, as showed in Figure 5 and reported in Table 1. The plasma density now fluctuates by approximately 7% as highlighted by the smaller range of the shadowed area and, overall, it reaches smoother values (up to  $1\text{--}1.3 \times 10^{17} \text{ cm}^{-3}$ ) along the fraction of the capillary structure shown in Figure 5. Moreover, besides the enhanced uniformity of the plasma between the two electrodes, a strongly reduced fluctuations of the outer plumes is noticeable.

**Table 1.** Data regarding the plasma density and its rising edge shot-to-shot stability with and without the laser-triggering technique.

Measurements	Voltage	Instability No Triggering	Instability Laser ON	Instability DC ON
Density Amplitude	5 kV	~20%	~7%	~7%
Density Amplitude	6 kV	~20%	~7%	~7%
Density Amplitude	7 kV	~10%	~7%	~7%
Shot-to-shot stability	5 kV	800 ns	5 ns	5.6 ns
Shot-to-shot stability	6 kV	220 ns	4 ns	4.1 ns
Shot-to-shot stability	7 kV	83 ns	1.8 ns	2.8 ns

The implementation of both methods gives a similar result regarding the stabilization of the current waveform and the uniformity of the longitudinal plasma density. Finally, an additional measurement regarding the time-jittering minimization, by the two triggering techniques, has been performed.

In Figure 6, the time-jittering with the two different triggering methods is reported. It is noticeable that without any stabilization method the time-jittering is in the  $\mu\text{s}$ -range (orange line). While, applying both methods we noticed a minimization of the jitter down to the ns-range, being able to stabilize the discharge until 3 kV near the breakdown level. The two methods combined do not produce any further minimization of the jittering. In Figure 7, an additional study has been performed to fully characterize the DC-triggering method influence. A current scan has been performed, from 70 pC to 15 pC, at the extreme configurations of the discharge voltages operational-range for 4 kV, unstable configuration near the breakdown level, and 9 kV, quasi-stable configuration, adopting just the DC-triggering configuration. It is retrieved that the time-jitter is almost constant as a function of the charge for 9 kV ( $\sim 2$  ns), while for a 4 kV discharge it is almost constant ( $\sim 16$  ns) until 40 pC and then is slightly degraded ( $\sim 3$  ns reaching  $\sim 20$  ns) until 15 pC.

**Figure 6.** Time-jitter measurements. Time-jittering of the discharge waveform without any stabilization method (red line), minimized by the laser-trigger technique (blue dashed-dotted line), by the DC-trigger technique (blue dashed line) and with both method combined (blue dotted line).

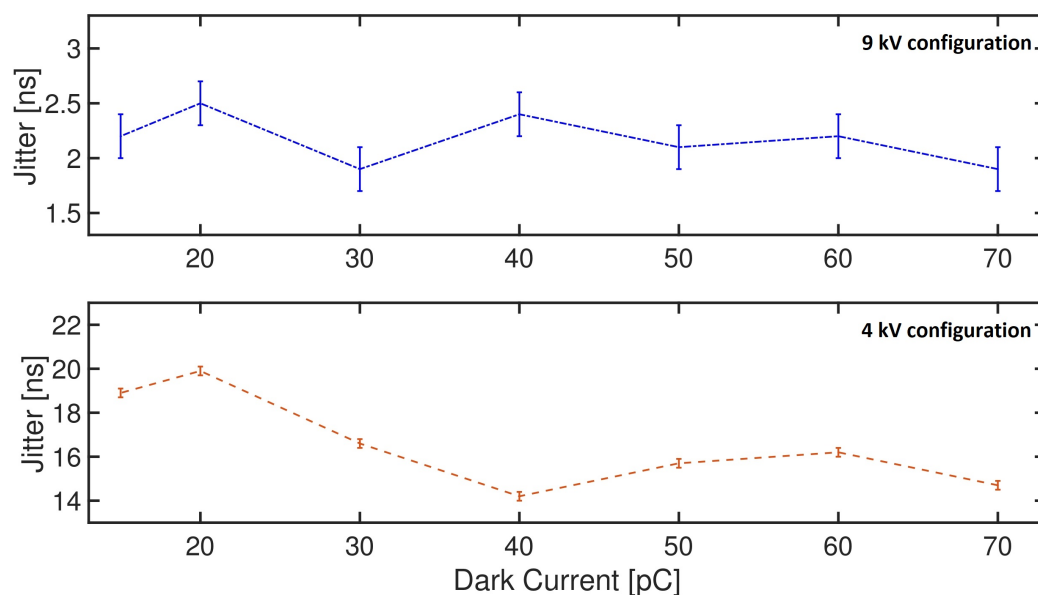


**Figure 7.** Time-jitter measurements. Time-jittering of the discharge waveform minimized by the DC-trigger technique at 9 kV configuration (**top**) and at 4 kV configuration (**bottom**).

#### 4. Conclusions

In conclusion, the improvements provided by a pre-ionizing technique, both driven by a laser pulse or by the LINAC generated dark current, regarding the optimization of a plasma device, namely, a gas-filled discharge-capillary are reported and extensively discussed. The goal was to demonstrate the reduction of the jitter sources and, in turn, the optimization of the plasma source becoming a symmetrical stable accelerating environment, even when the starting configuration is an highly unstable non-symmetrical one, for future accelerator machines employing plasma-based devices. Comparing the plasma generated by only applying a high-voltage discharge and the one created with an additional triggering technique, we found a clear enhancement of the overall stability. Both techniques are valid approach but, for the first time to our knowledge, we demonstrate that the dark-current triggering method, requiring less complex setup, achieves comparable results to other techniques to fulfill the plasma stabilization. This approach allows to generate stable beams, as required by user-oriented applications, paving the way toward the development of next-generation compact plasma-based accelerators.

**Author Contributions:** M.G., R.P., M.F. and A.Z. planned and managed the experiment with inputs from all the co-authors. A.B. and S.A. provided the plasma characterization. A.C. and V.S. realized the beam diagnostics. V.L. designed the capillary and managed the vacuum system. M.P.A., F.V., G.C., M.G. and M.D.G. managed the photo-cathode and the stabilization laser system. M.G., A.B. and Y.R. carried out the data analysis. M.G. and R.P. wrote the manuscript. All authors have read and agreed to the published version of the manuscript.

**Funding:** This research has been partially funded by the EU Commission in the Seventh Framework Program, Grant Agreement 312453-EuCARD-2, the European Union Horizon 2020 research and innovation program, Grant Agreement No. 653782 (EuPRAXIA) and the INFN with the GRANT73/PLADIP grant. The work of one of us (A.Z.) was partially supported by ISF foundation.

**Acknowledgments:** The authors thank D. Pellegrini, U. Frascaco and E. Gaspari for the realization of the HV discharge pulser and M. Del Franco for providing the layout of the SPARC\_LAB photo-injector.

**Conflicts of Interest:** The authors declare no conflict of interest.

#### References

1. Tajima, T.; Dawson, J.M. Laser electron accelerator. *Phys. Rev. Lett.* **1979**, *43*, 267. [[CrossRef](#)]
2. Ackermann, W.A.; Asova, G.; Ayvazyan, V.; Azima, A.; Baboi, N.; Bähr, J.; Balandin, V.; Beutner, B.; Brandt, A.; Bolzmann, A.; et al. Operation of a free-electron laser from the extreme ultraviolet to the water window. *Nat. Photonics* **2007**, *1*, 336–342. [[CrossRef](#)]



3. Emma, P.; Akre, R.; Arthur, J.; Bionta, R.; Bostedt, C.; Bozek, J.; Brachmann, A.; Bucksbaum, P.; Coffee, R.; Decker, F.J.; et al. First lasing and operation of an ångstrom-wavelength free-electron laser. *Nat. Photonics* **2010**, *4*, 641. [[CrossRef](#)]
4. Petrillo, V.; Anania, M.; Artioli, M.; Bacci, A.; Bellaveglia, M.; Chiadroni, E.; Cianchi, A.; Ciocci, F.; Dattoli, G.; Di Giovenale, D.; et al. Observation of time-domain modulation of free-electron-laser pulses by multi-peaked electron-energy spectrum. *Phys. Rev. Lett.* **2013**, *111*, 114802. [[CrossRef](#)] [[PubMed](#)]
5. Schoenlein, R.W.; Leemans, W.; Chin, A.; Volfbeyn, P. Femtosecond X-ray pulses at 0.4 microns generated by 90 degree Thomson scattering: A tool for probing the structural dynamics of materials. *Science* **1996**, *274*, 236. [[CrossRef](#)]
6. Chiadroni, E.; Bacci, A.; Bellaveglia, M.; Boscolo, M.; Castellano, M.; Cultrera, L.; Di Pirro, G.; Ferrario, M.; Ficcadenti, L.; Filippetto, D.; et al. The SPARC linear accelerator based terahertz source. *Appl. Phys. Lett.* **2013**, *102*, 094101. [[CrossRef](#)]
7. Bourhis, J.; Sozzi, W.J.; Jorge, P.G.; Gaide, O.; Bailat, C.; Duclos, F.; Patin, D.; Ozsahin, M.; Bochud, F.; Germond, J.F.; et al. Treatment of a first patient with FLASH-radiotherapy. *Radiother. Oncol.* **2019**, *139*, 18–22. [[CrossRef](#)] [[PubMed](#)]
8. Van Tilborg, J.; Steinke, S.; Geddes, C.; Matlis, N.; Shaw, B.; Gonsalves, A.; Huijts, J.; Nakamura, K.; Daniels, J.; Schroeder, C.; et al. Active plasma lensing for relativistic laser-plasma-accelerated electron beams. *Phys. Rev. Lett.* **2015**, *115*, 184802. [[CrossRef](#)]
9. Panofsky, W.K.H.; Baker, W. A Focusing Device for the External 350-Mev Proton Beam of the 184-Inch Cyclotron at Berkeley. *Rev. Sci. Instrum.* **1950**, *21*, 445–447. [[CrossRef](#)]
10. Pompili, R.; Anania, M.; Bellaveglia, M.; Biagioni, A.; Bini, S.; Bisesto, F.; Brentegani, E.; Cardelli, F.; Castorina, G.; Chiadroni, E.; et al. Focusing of high-brightness electron beams with active-plasma lenses. *Phys. Rev. Lett.* **2018**, *121*, 174801. [[CrossRef](#)]
11. Leemans, W.; Gonsalves, A.; Mao, H.S.; Nakamura, K.; Benedetti, C.; Schroeder, C.; Tóth, C.; Daniels, J.; Mittelberger, D.; Bulanov, S.; et al. Multi-GeV electron beams from capillary-discharge-guided subpetawatt laser pulses in the self-trapping regime. *Phys. Rev. Lett.* **2014**, *113*, 245002. [[CrossRef](#)] [[PubMed](#)]
12. Faure, J.; Rechatin, C.; Norlin, A.; Lifschitz, A.; Glinec, Y.; Malka, V. Controlled injection and acceleration of electrons in plasma wakefields by colliding laser pulses. *Nature* **2006**, *444*, 737. [[CrossRef](#)]
13. Leemans, W.; Nagler, B.; Gonsalves, A.; Tóth, C.; Nakamura, K.; Geddes, C.; Esarey, E.; Schroeder, C.; Hooker, S. GeV electron beams from a centimetre-scale accelerator. *Nat. Phys.* **2006**, *2*, 696. [[CrossRef](#)]
14. Geddes, C.; Toth, C.; Van Tilborg, J.; Esarey, E.; Schroeder, C.B.; Bruhwiler, D.; Nieter, C.; Cary, J.; Leemans, W.P. High-quality electron beams from a laser wakefield accelerator using plasma-channel guiding. *Nature* **2004**, *431*, 538. [[CrossRef](#)] [[PubMed](#)]
15. Faure, J.; Glinec, Y.; Pukhov, A.; Kiselev, S.; Gordienko, S.; Lefebvre, E.; Rousseau, J.-P.; Burgy, F.; Malka, V. A laser-plasma accelerator producing monoenergetic electron beams. *Nature* **2004**, *431*, 541. [[CrossRef](#)]
16. Blumenfeld, I.; Clayton, C.E.; Decker, F.J.; Hogan, M.J.; Huang, C.; Ischebeck, R.; Iverson, R.; Joshi, C.; Katsouleas, T.; Kirby, N.; et al. Energy doubling of 42GeV electrons in a metre-scale plasma wakefield accelerator. *Nature* **2007**, *445*, 741–744. [[CrossRef](#)]
17. Litos, M.; Adli, E.; An, W.; Clarke, C.; Clayton, C.; Corde, S.; Delahaye, J.; England, R.; Fisher, A.; Frederico, J.; et al. High-efficiency acceleration of an electron beam in a plasma wakefield accelerator. *Nature* **2014**, *515*, 92–95. [[CrossRef](#)]
18. Adli, E.; Ahuja, A.; Apsimon, O.; Apsimon, R.; Bachmann, A.M.; Barrientos, D.; Batsch, F.; Bauche, J.; Olsen, V.B.; Bernardini, M.; et al. Acceleration of electrons in the plasma wakefield of a proton bunch. *Nature* **2018**, *561*, 363–367. [[CrossRef](#)]
19. Sprangle, P.; Esarey, E.; Krall, J. Laser driven electron acceleration in vacuum, gases, and plasmas. *Phys. Plasmas* **1996**, *3*, 2183–2190. [[CrossRef](#)]
20. Hogan, M.; Raubenheimer, T.; Seryi, A.; Muggli, P.; Katsouleas, T.; Huang, C.; Lu, W.; An, W.; Marsh, K.; Mori, W.; et al. Plasma wakefield acceleration experiments at FACET. *New J. Phys.* **2010**, *12*, 055030. [[CrossRef](#)]
21. Hidding, B.; Beaton, A.; Boulton, L.; Corde, S.; Doepp, A.; Habib, F.A.; Heinemann, T.; Irman, A.; Karsch, S.; Kirwan, G.; et al. Fundamentals and applications of hybrid lwfa-pwfa. *Appl. Sci.* **2019**, *9*, 2626. [[CrossRef](#)]
22. Rocca, J.J.; Clark, D.; Chilla, J.; Shlyaptsev, V. Energy extraction and achievement of the saturation limit in a discharge-pumped table-top soft X-ray amplifier. *Phys. Rev. Lett.* **1996**, *77*, 1476. [[CrossRef](#)] [[PubMed](#)]
23. Gonsalves, A.; Nakamura, K.; Daniels, J.; Benedetti, C.; Pieronek, C.; De Raadt, T.; Steinke, S.; Bin, J.; Bulanov, S.; Van Tilborg, J.; et al. Petawatt laser guiding and electron beam acceleration to 8 GeV in a laser-heated capillary discharge waveguide. *Phys. Rev. Lett.* **2019**, *122*, 084801. [[CrossRef](#)] [[PubMed](#)]
24. Bobrova, N.; Esaulov, A.; Sakai, J.I.; Satorov, P.; Spence, D.; Butler, A.; Hooker, S.; Bulanov, S. Simulations of a hydrogen-filled capillary discharge waveguide. *Phys. Rev. E* **2001**, *65*, 016407. [[CrossRef](#)]
25. Ferrario, M.; Alesini, D.; Anania, M.; Bacci, A.; Bellaveglia, M.; Bogdanov, O.; Boni, R.; Castellano, M.; Chiadroni, E.; Cianchi, A.; et al. SPARC\_LAB present and future. *Nucl. Instrum. Methods Phys. Res. Sect. Beam Interact. Mater. Atoms* **2013**, *309*, 183–188. [[CrossRef](#)]
26. Villa, F.; Cialdi, S.; Anania, M.; Gatti, G.; Giorgianni, F.; Pompili, R. Laser pulse shaping for multi-bunches photoinjectors. *Nucl. Instrum. Methods Phys. Res. Sect. Accel. Spectrometers Detect. Assoc. Equip.* **2014**, *740*, 188–192. [[CrossRef](#)]
27. Ferrario, M.; Alesini, D.; Bacci, A.; Bellaveglia, M.; Boni, R.; Boscolo, M.; Castellano, M.; Chiadroni, E.; Cianchi, A.; Cultrera, L.; et al. Experimental demonstration of emittance compensation with velocity bunching. *Phys. Rev. Lett.* **2010**, *104*, 054801. [[CrossRef](#)]
28. Pompili, R.; Anania, M.; Bellaveglia, M.; Biagioni, A.; Bisesto, F.; Chiadroni, E.; Cianchi, A.; Croia, M.; Curcio, A.; Di Giovenale, D.; et al. Beam manipulation with velocity bunching for PWFA applications. *Nucl. Instrum. Methods Phys. Res. Sect. Accel. Spectrometers Detect. Assoc. Equip.* **2016**, *829*, 17–23. [[CrossRef](#)]

29. Curcio, A.; Bisesto, F.; Costa, G.; Biagioni, A.; Anania, M.P.; Pompili, R.; Ferrario, M.; Petrarca, M. Modeling and diagnostics for plasma discharge capillaries. *Phys. Rev. E* **2019**, *100*, 053202. [[CrossRef](#)]
30. Griem, H.R.; Kolb, A.C.; Shen, K. Stark broadening of hydrogen lines in a plasma. *Phys. Rev.* **1959**, *116*, 4. [[CrossRef](#)]
31. Biagioni, A.; Alesini, D.; Anania, M.; Bellaveglia, M.; Bini, S.; Bisesto, F.; Brentegani, E.; Chiadroni, E.; Cianchi, A.; Coiro, O.; et al. Temperature analysis in the shock waves regime for gas-filled plasma capillaries in plasma-based accelerators. *J. Instrum.* **2019**, *14*, C03002. [[CrossRef](#)]
32. Jang, D.; Kim, M.; Nam, I.; Uhm, H.; Suk, H. Density evolution measurement of hydrogen plasma in capillary discharge by spectroscopy and interferometry methods. *Appl. Phys. Lett.* **2011**, *99*, 141502. [[CrossRef](#)]
33. Griem, H. *Spectral Line Broadening by Plasmas*; Elsevier: Amsterdam, The Netherlands, 2012.
34. Bednar, N.J.; Walewski, J.W.; Sanders, S.T. Assessment of multiphoton absorption in inert gases for the measurement of gas temperatures. *Appl. Spectrosc.* **2006**, *60*, 246–253. [[CrossRef](#)] [[PubMed](#)]
35. Bobrova, N.; Sasorov, P.; Benedetti, C.; Bulanov, S.; Geddes, C.; Schroeder, C.; Esarey, E.; Leemans, W. Laser-heater assisted plasma channel formation in capillary discharge waveguides. *Phys. Plasmas* **2013**, *20*, 020703. [[CrossRef](#)]
36. Loveless, A.M.; Garner, A.L. A universal theory for gas breakdown from microscale to the classical Paschen law. *Phys. Plasmas* **2017**, *24*, 113522. [[CrossRef](#)]